Aust. J. Math. Anal. Appl.
Vol. **22** (2025), No. 2, Art. 3, 10 pp.
AJMAA

STRONG AND FRAGILE CHAOS IN A NEW TWO-DIMENSIONAL QUADRATIC PIECEWISE SMOOTH MAP AND ITS APPLICATIONS

ABDELLAH MENASRI, ABDELKADIR SOUDANI

Received 21 December, 2024; accepted 03 July, 2025; published 22 August, 2025.

HIGHER NATIONAL SCHOOL OF FORESTS, KHENCHELA, SYSTEM DYNAMICS AND CONTROL LABORATORY, DEPARTMENT OF MATHEMATICS AND INFORMATICS, OUM EL BOUAGHI UNIVERSITY, ALGERIA.
menasri.abdellah@ensf.dz

ICOSI LABORATORY, DEPARTMENT OF MATHEMATICS AND INFORMATICS, COLLEGE OF SCIENCE AND TECHNOLOGY, KHENCHELA UNIVERSITY, KHENCHELA 40004, ALGERIA.
soudaniabdelkadir@yahoo.com

ABSTRACT. The Henon and Lozi maps are among the most widely used in physics applications due to their ability to generate two chaotic attractors for specific values of their bifurcation parameters. In this study, I propose a new 2D smooth piecewise quadratic map created by merging the two maps. We demonstrate that this map exhibits both strong and fragile chaotic behavior for varying values of the bifurcation parameters a and b. The new map reveals distinct chaotic attractors, displaying both strong and fragile chaos for certain values of these parameters. Consequently, this map produces two chaotic attractors one fragile and the other strong highlighting the rich diversity of dynamic behavior.

Key words and phrases: Henon and Lozi maps; New quadratic piecewise smooth map; Border collision bifurcations; Fragile chaos and Strong chaos; New chaotic attractor; Applications.

2010 *Mathematics Subject Classification.* 37E05, 37G05, 37G10 .

ISSN (electronic): 1449-5910

1. INTRODUCTION

Quadratic smooth maps and piecewise smooth maps are fundamental tools in mathematical modeling, offering powerful frameworks for analyzing complex dynamical systems across physics, engineering, economics, and computational sciences. Due to their ability to capture nonlinear phenomena, such as chaos, bifurcations, and fractal structures, these maps have attracted significant research interest.

For instance, Zeraoulia & Sprott [1] introduced a novel piecewise smooth planar map that generalizes the Hénon and Lozi systems, unifying them as extreme cases within a broader class of chaotic transitions. Similarly, Menasri [2] investigated Lozi maps incorporating the max function, demonstrating robust chaotic behavior under specific parameter regimes. In economics, discontinuous 2D maps have been employed to model growth dynamics with optimal savings and behavioral shifts [10], where stability conditions for fixed points (Solow and Pasinetti equilibria) were derived, alongside analyses of bifurcation structures and chaotic attractors.

These studies underscore the versatility of smooth and piecewise smooth maps in characterizing diverse dynamical behaviors, motivating further exploration of their theoretical and applied implications.

2. BORDER COLLISION BIFURCATIONS

Border collision bifurcations (BCBs) [9] occur in piecewise smooth dynamical systems, where the state space is partitioned into distinct regions governed by different smooth functions. When a system trajectory crosses the boundary between these regions, the dynamics may undergo a sudden qualitative change, leading to a bifurcation. Unlike classical bifurcations in smooth systems, BCBs arise specifically due to discontinuities in the system's Jacobian at the boundary, making them unique to piecewise smooth models. The triggering parameter for BCBs is often linked to the system's initial conditions or the parameters defining the boundary itself.

BCBs are broadly classified into two types:

Period-Adding Bifurcations: As a parameter varies, periodic orbits emerge at the boundary, with their period incrementally increasing (e.g., period-doubling or tripling cascades). This results in a structured sequence of stable periodic solutions.

Period-Increasing Bifurcations: The system transitions from chaotic to periodic behavior, with the orbit period growing monotonically as the parameter changes.

These bifurcations are pivotal in chaos theory and nonlinear dynamics, enabling phenomena such as the abrupt onset of chaos, stabilization of periodic orbits, and complex attractor metamorphoses. Their practical relevance spans engineering applications, including power electronics, digital control systems, and communication networks, where piecewise smooth models describe switching behaviors. By elucidating the mechanisms of BCBs, researchers gain critical insights into system stability and controllability, advancing both theoretical understanding and real-world problem-solving in complex dynamical systems.

3. ROBUST AND FRAGILE CHAOS IN DYNAMICAL SYSTEMS

Robust chaos describes a form of chaotic dynamics that remains stable under variations in system parameters, initial conditions, or structural perturbations. This resilience arises from the presence of structurally stable attractors, which maintain chaotic behavior despite external disturbances. Key features of robust chaos include:

1. Persistence of chaos across a broad parameter range,
2. Insensitivity to perturbations,
3. Frequent occurrence in systems with piecewise-smooth dynamics or strong nonlinearities, such as the Lozi and Belykh maps.

In contrast, **fragile chaos** is highly sensitive to minor system modifications, with chaotic behavior collapsing into periodic or fixed-point dynamics under slight parameter variations. This form of chaos emerges in systems where attractors lack structural stability and depend critically on precise configurations. Characteristics include:

1. Rapid disappearance of chaos under perturbations,
2. Extreme dependence on specific parameter values,
3. Prevalence in finely tuned systems, such as weakly dissipative or high-dimensional oscillators. The distinction between these regimes highlights the interplay between nonlinearity, stability, and parametric sensitivity in chaotic systems.

4. A NEW TWO-DIMENSIONAL QUADRATIC PIECEWISE-SMOOTH MAP

The Henon map is a prototypical two-dimensional, invertible iterated map that exhibits a chaotic attractor [5], [7]. It serves as a simplified model of the Poincaré map for the Lorenz system, which was proposed by M. Henon in 1976 and is given by:

$$H(x;y) = \begin{pmatrix} 1 - ax^2 + by \\ x \end{pmatrix}$$

A modification of the first equation in the Henon map was made by Lozi in 1980, who replaced the x^2 term with $|x|$. This modification resulted in a new piecewise smooth map, given by:

$$L(x;y) = \begin{pmatrix} 1 - a\,|x| + by \\ x \end{pmatrix}$$

It has been proven that both maps exhibit chaotic behavior [1], [8]. Their chaotic attractors are illustrated in Figures (1) and (2).

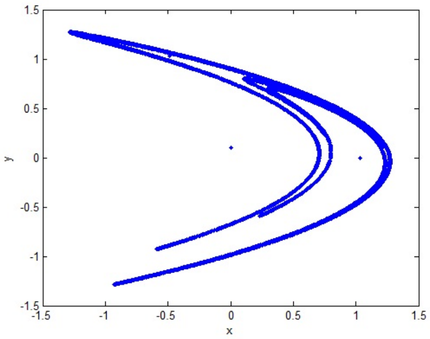

Figure 1: The chaotic attractor of Henon, $a = 1.4, b = 0.3$..

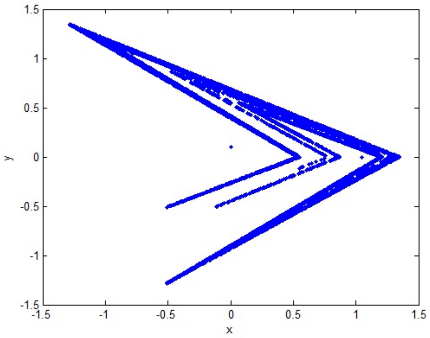

Figure 2: The chaotic attractor of Lozi, $a = 1.7, b = 0.5$.

Consider the following two-dimensional quadratic Piecewise-Smooth map:

$$M(x;y) = \begin{pmatrix} 1 - a(|x| + x^2) + by \\ x \end{pmatrix}, \tag{4.1}$$

where a and b are positive parameters, $|x|$ represents the absolute value function, and the map is piecewise smooth due to the non-differentiability of the absolute value term. The system exhibits a border collision bifurcation when the trajectory of the system crosses the boundary between different regions of behavior, causing a qualitative change in the system's dynamics.

We can express the map (1) in the following form:

$$M(x;y) = \begin{cases} \begin{pmatrix} 1 - ax + by - ax^2 \\ x \end{pmatrix} & \text{if } (x;y) \in R_A \\ \begin{pmatrix} 1 + ax + by - ax^2 \\ x \end{pmatrix} & \text{if } (x;y) \in R_B \end{cases}, \tag{4.2}$$

where $R_A = \{(x;y) \in \mathbb{R}^2 : x \geq 0\}, R_B = \{(x;y) \in \mathbb{R}^2 : x \leq 0\}$.

The map (1) has two fixed points, one on R_B (left side) and the other on R_A (right side), following the sign of parameter a. The fixed points are given by the following cases:

Case.1: if $a < 0$,

$$P_A\left(\frac{-(1+a-b)+\sqrt{(1+a-b)^2+4a}}{2a}; \frac{-(1+a-b)+\sqrt{(1+a-b)^2+4a}}{2a}\right),$$

$$P_B\left(\frac{-(1-a-b)-\sqrt{(1-a-b)^2+4a}}{2a}; \frac{-(1-a-b)-\sqrt{(1-a-b)^2+4a}}{2a}\right).$$

Case.2: if $a > 0$

$$P_A\left(\frac{-(1+a-b)-\sqrt{(1+a-b)^2+4a}}{2a}; \frac{-(1+a-b)-\sqrt{(1+a-b)^2+4a}}{2a}\right),$$

$$P_B\left(\frac{-(1-a-b)+\sqrt{(1-a-b)^2+4a}}{2a}; \frac{-(1-a-b)+\sqrt{(1-a-b)^2+4a}}{2a}\right).$$

We note that the nature of the border collision bifurcation depends on the local behavior of the map in the neighborhood of the fixed point [9], [4]. Therefore, we focus on the piecewise linear approximation on the sides of the border (R_A and R_B). It has been shown that a normal form for the piecewise system in the neighborhood of a fixed point on the border (i.e., P_A on R_A and P_B on R_B) can be expressed as:

$$\begin{pmatrix} x_{n+1} \\ y_{n+1} \end{pmatrix} = \begin{cases} \begin{pmatrix} \tau_A & 1 \\ -\delta_A & 0 \end{pmatrix} \begin{pmatrix} x_n \\ y_n \end{pmatrix} + \mu \begin{pmatrix} 1 \\ 0 \end{pmatrix}, x_n \leq 0 \\ \begin{pmatrix} \tau_B & 1 \\ -\delta_B & 0 \end{pmatrix} \begin{pmatrix} x_n \\ y_n \end{pmatrix} + \mu \begin{pmatrix} 1 \\ 0 \end{pmatrix}, x_n \geq 0 \end{cases} \tag{4.3}$$

Where μ is a bifurcation parameter and $\tau_A, \tau_B, \delta_A, \delta_B$ are the traces and determinants for the two matrix (3) and (4) evaluated to P_A and P_B respectively. Hence, we have

$$\begin{cases} \tau_A = -a \\ \tau_B = a \\ \delta_A = \delta_B = -b \end{cases} \tag{4.4}$$

5. CLASSIFICATION OF BORDER COLLISION BIFURCATIONS

The following two tables shows the classification of the border collision bifurcations $[9]$ of the map (1) according to the two bifurcation parameters a and b.

Case.1: if $a < 0$,

Fixed points	Type	Condition
P_A	a flip saddle.	$1 - b < a < 0, b > 1.$
P_B	a flip saddle.	$a < \min(0, b - 1).$
P_B	a flip attractors.	$b - 1 < a < -2\sqrt{-b}, b \leq 0, b \neq -1.$
P_A, P_B	a spiral attractor.	$-2\sqrt{-b} < a < 0, b < 0.$
P_A	a regular attractor.	$b - 1 < a < -2\sqrt{-b}, b \leq 0, b \neq -1.$
P_A	a regular saddle.	$a < \min(0, b - 1).$
P_B	a regular saddle.	$1 - b < a < 0, b > 1.$

Case.2: if $a > 0$,

Fixed points	Type	Condition
P_A	a flip saddle.	$a > \max(1 - b; 0).$
P_B	a flip saddle.	$0 < a < b - 1, b > 1.$
P_A	a flip attractors.	$2\sqrt{-b} < a < 1 - b, b \leq 0, b \neq -1.$
P_A, P_B	a spiral attractor.	$0 < a < 2\sqrt{-b}, b < 0.$
P_B	a regular attractor.	$2\sqrt{-b} < a < 1 - b, b \leq 0, b \neq -1.$
P_A	a regular saddle.	$0 < a < b - 1, b > 1.$
P_B	a regular saddle.	$a > \max(1 - b, 0).$

5.1. **Numerical simulation .**
The numerical simulation using MATLAB reveals that the map (1) exhibits chaotic behavior depending on the values of the two bifurcation parameters, a and b. When $a = 0.8$ and $b = 0.3$, with the initial condition $(0.1; 0.1)$, a new chaotic attractor is observed, as shown in figures (3) and (4). This attractor exhibits strong chaotic behavior, indicating robust chaos. The Lyapunov exponents are $\lambda_1 = 0.495$ and $\lambda_2 = -1.699$. The Lyapunov dimension of the map (1) is calculated as follows: $D_L = 1 + \frac{\lambda_1}{|\lambda_2|} \approx 1.291$.

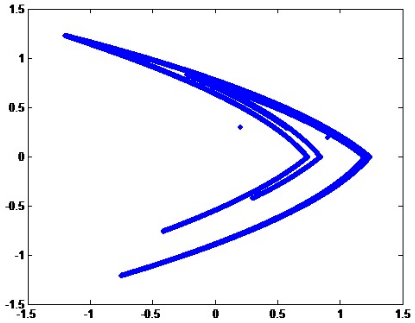

Figure 3: The chaotic attractor of the map (1) *for* $a = 0.8, b = 0.3$.

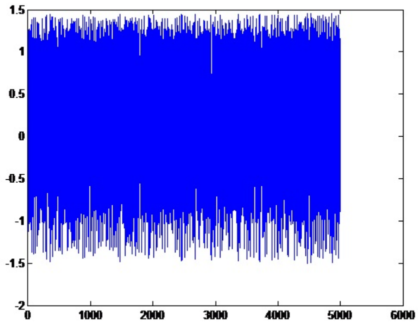

Figure 4: Time series x_n *corresponding to the initial condition* $(0, 0)$ *for* $a = 0.8, b = 0.3$.

For the same initial condition and with $a = 0.7$ and $b = 0.5$, we observe another new chaotic attractor, as shown in figures (5) and (6). This attractor also exhibits delicate chaotic behavior, indicating fragile chaos. Additionally, we calculated two Lyapunov exponents with values $\lambda_1 = 0.12$ and $\lambda_2 = -0.82$. Therefore, the Lyapunov dimension is approximately $D_L \approx 1.146$. These results confirm that the map (1) exhibits high sensitivity to the initial conditions, and its attractor is strange [6]. Furthermore, the numerical simulations show that after a sufficient number of iterations, the attractor remains bounded due to $\max(x_n) = \max(y_n) < 1.5$ and $\min(x_n) = \min(y_n) > -2$.

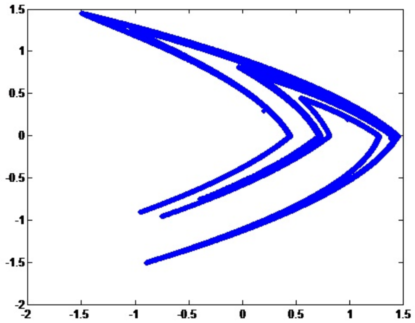

Figure 5: The chaotic attractor of the map (1) *for* $a = 0.7, b = 0.5$.

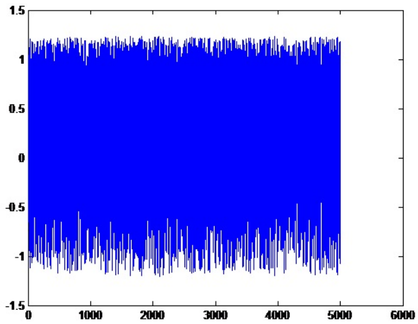

Figure 6: Time series x_n *corresponding to the initial condition* $(0, 0)$ *for* $a = 0.7, b = 0.5$.

Furthermore, for two values of the parameter b, namely $b = 0.3$ and $b = 0.5$, with $0 < a < 1$, numerical simulations yield the bifurcation diagrams shown in Figures (7) and (8). These diagrams illustrate that the dynamics of map (1) vary significantly with changes in the bifurcation parameter a, displaying different regimes of stability, bifurcation structures, and chaotic behavior. In particular, Figure (7), corresponding to $b = 0.3$, demonstrates robust chaos, characterized by a persistent chaotic regime with no periodic windows over the considered range of a. In contrast, Figure (8), associated with $b = 0.5$, exhibits fragile chaos, where chaotic regions are interspersed with periodic windows, indicating sensitive dependence on parameter variations.

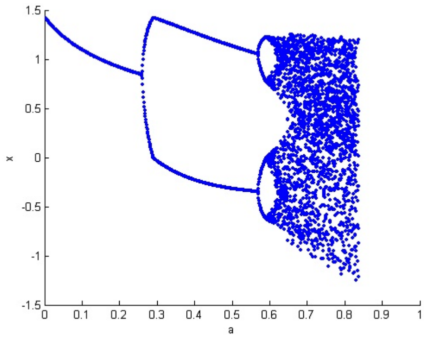

Figure 7: The diagram bifurcation of the map (1) *for* $0 < a < 1, b = 0.3$.

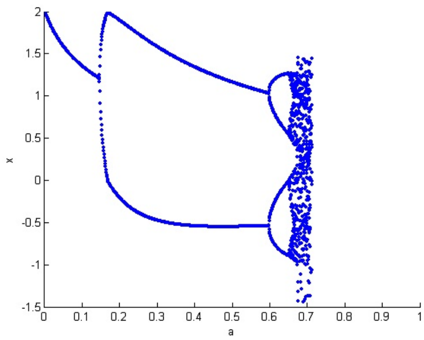

Figure 8: The diagram bifurcation of the map (1) *for* $0 < a < 1, b = 0.5$.

On the other hand, the $0 - 1$ test for chaos confirms chaotic dynamics in both parameter configurations: $a = 0.8, b = 0.3$ and $a = 0.7, b = 0.5$.

In the first case $(a = 0.8, b = 0.3)$, the $ln(Pn)$ curve displays a pronounced asymptotic growth with a slope of approximately 1.26, indicating strong quadratic diffusion. This rapid divergence of nearby trajectories is a hallmark of deterministic chaos and reflects robust chaos, as depicted in Figure (9).

In the second case $(a = 0.7, b = 0.5)$, the $ln(Pn)$ curve also grows with a positive slope of about 0.71, confirming the presence of chaotic behavior. However, the reduced slope and less pronounced diffusion suggest fragile chaos, where chaotic behavior coexists with intermittent stability, as shown in Figure (10).

In both scenarios, the system exhibits long-term unpredictability due to its sensitivity to initial conditions, despite being governed by deterministic rules. These observations underline the contrasting natures of robust and fragile chaos under different parameter regimes.

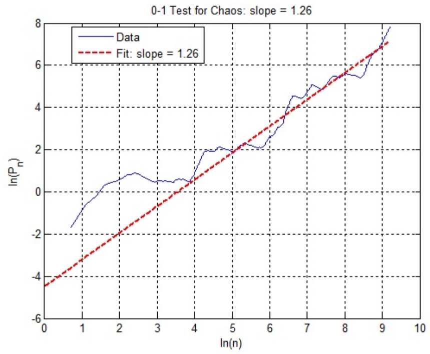

Figure 9: The 0-1 test for chaos of the Map (1): $a = 0.8$ *and* $b = 0.3$.

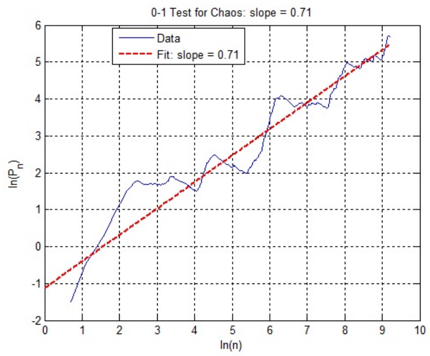

Figure 10: The 0-1 test for chaos of the Map (1): $a = 0.7$ *and* $b = 0.5$.

5.2. **Some concrete applications where map (1) can be utilized and adapted to the real world.** The concealment of information is a major concern for countries worldwide. Consequently, various encryption techniques have been developed to render information incomprehensible to unauthorized parties lacking access to a secret key. These techniques find applications in both commercial and personal domains and have a long history dating back to antiquity, with primitive methods such as the scytale or Caesar cipher.

Over time, these methods evolved into masking techniques, automated machines, and now, modern computational encryption. The advent of computers has introduced remarkable computational power, leading to the development of complex encryption techniques. Among these advancements, the security of modern communications largely relies on the complex dynamic behaviors exhibited by chaotic systems.

Chaos, as a deterministic phenomenon, allows for the decoding of data by leveraging its intrinsic properties. However, to ensure robust security, the use of strong chaos is essential. Unlike fragile chaos, which can disappear under small perturbations, strong chaos offers critical stability and resilience against parameter variations or external attacks. Communication systems based on strong chaos efficiently exploit these characteristics, making encryption both secure and reliable.

The two-dimensional piecewise smooth quadratic map studied in this article exhibits distinctive properties, particularly robust chaotic behavior, suggesting its potential for numerous real-world applications, especially in secure encryption. These properties ensure that, even in the presence of disturbances, the data remains protected, underscoring the importance of strong chaos in modern encryption systems.

Conclusion 1. *In this paper, we introduced a new piecewise smooth quadratic two-dimensional map. We have demonstrated that this map exhibits chaotic behavior and yields two new chaotic attractors for specific values of the bifurcation parameters a and b. Furthermore, this map uniquely combines strong chaos and fragile chaos, a critical property that enhances its versatility and applicability. The coexistence of strong and fragile chaos ensures robustness under parameter variations while maintaining high sensitivity, making it particularly suitable for advanced applications. This map holds significant potential for various applications, especially in electronics and encryption within the fields of media and telecommunications. Its chaotic properties provide a robust framework for secure communication and signal processing, underscoring its importance in real-world scenarios.*

REFERENCES

[1] A. ALAOUI, M.A, CA. ROBERT, Ce. Grebogi, *Dynamics of a Hénon-Lozi map, Proc. Chaos . J. Chaos, Solitons and Fractals,* **12** (2010), pp. 2323-2341.

[2] A. MENASRI, Lozi Maps With max *Function and its application, Australian Journal of Mathematical Analysis and Applications*, **20**(2023), Art 6, pp. 13

[3] E. ZERAOULIA, J. C. Sprott, A uni.ed *piecewise smooth chaotic mapping that contains the Hénon and the Lozi systems, Annual Review of Chaos Theory, Bifurcations and Dynamical Systems*, 1(2012), pp. 50-60.

[4] E. ZERALOUIA, J. C. SPROTT, *On the robustness of chaos in dynamical, Frontiers of physics in China*, **3**(2018), pp. 195-204.

[5] F. R. MAOROTTO, *Chaotic behavior in the Hénon mapping, Journal Com Math. Phys*, **68**(1979), pp. 187-194.

[6] M. ANDRECUT, M. K. ALI, *On the occurrence of robust chaos in a smooth system, Modern Physics Letters B*, **15**(2001), pp. 391-395.

[7] M. BENEDICJKS, L. CARLESON, *The dynamics of the Hénon maps, Annals of Mathematics*, **133**(1979), pp. 1-25.

[8] M. MISIUREWICZ, *Strange attractor for the Lozi-mapping in Nonlinar dynamics*, Annals of the New York Academy of Sciences, **357**(1980), pp. 348-358.

[9] S. BANERJEE, C. GREBOJI, *Border collision bifurcations in two-dimensional piece-wise smooth maps*, Interdisciplinary Journal of Nonlinear Science, **59**(1999), pp. 4052-4061.

[10] IRYNA SUSHKO, Pasquale Commendatore and Ingrid Kubin, *Codimension-two border collision bifurcation in a two-class growth model with optimal saving and switch in behavior, Nonlinear Dynamics*, **102**(2020), pp. 1071-1095.